Zeitschrift: Eclogae Geologicae Helvetiae
Herausgeber: Schweizerische Geologische Gesellschaft
Band: 84 (1991)
Heft: 2

Artikel: Tomographic image of the Pacific Slab under southern Alaska
Autor: Kissling, Eduard / Lahr, John C.
DOI: https://doi.org/10.5169/seals-166775

Nutzungsbedingungen
Die ETH-Bibliothek ist die Anbieterin der digitalisierten Zeitschriften. Sie besitzt keine Urheberrechte an den Zeitschriften und ist nicht verantwortlich für deren Inhalte. Die Rechte liegen in der Regel bei den Herausgebern beziehungsweise den externen Rechteinhabern. Siehe Rechtliche Hinweise.

Conditions d'utilisation
L'ETH Library est le fournisseur des revues numérisées. Elle ne détient aucun droit d'auteur sur les revues et n'est pas responsable de leur contenu. En règle générale, les droits sont détenus par les éditeurs ou les détenteurs de droits externes. Voir Informations légales.

Terms of use
The ETH Library is the provider of the digitised journals. It does not own any copyrights to the journals and is not responsible for their content. The rights usually lie with the publishers or the external rights holders. See Legal notice.

Download PDF: 19.03.2025

ETH-Bibliothek Zürich, E-Periodica, https://www.e-periodica.ch

Eclogae geol. Helv. 84/2: 297–315 (1991)

0012-9402/91/020297-19 $ 1.50 + 0.20/0
Birkhäuser Verlag, Basel

Tomographic image of the Pacific Slab under southern Alaska[1])

By Eduard Kissling[2]) and John C. Lahr[3])

ABSTRACT

Southern Alaska is characterized by high-seismic activity due to the subduction of the Pacific plate under the continental lithosphere of Alaska. A high quality data set of local earthquakes has been inverted to obtain a tomographic image of the three-dimensional (3D) velocity structure down to a depth of 200 km. Imaging this large area with a block size of 10 km by 10 km required that an approximate solution to the full inversion be used and therefore the results are preliminary. The dominant features in the tomographic image are elongated deep-reaching velocity anomalies striking SW-NE parallel to the volcanic arc. The largest continuous anomaly is a region of low P-wave velocity. This anomaly parallels and overlies the zone of relatively high P-wave velocity associated with the descending lithosphere. The maximum amplitudes of the P-wave velocity anomalies are +5% for the subducted slab and −10% for the areas of low velocity above the slab. In the southern part of Kenai Penninsula, where the high-velocity anomaly is well developed, the earthquakes are concentrated both in the crust and along a zone that includes the uppermost part of the high velocity anomaly and the region of high gradient between the high and the low P-wave velocity anomalies. Further to the north where the amplitude and the size of the high-velocity anomaly is reduced, the deepest portion of the seismogenic zone extends from within the gradient zone into the region of low velocity. First motion data for events within the Benioff-Wadati zone (BWZ) were used to determine composite focal mechanisms. The T-axis of these mechanisms tend to remain parallel to the dip of the BWZ as it increases from about 10 to 60 degrees. This pattern is consistent with BWZ earthquakes occurring within a contiguous plate which is sinking due to gravitational forces and acting as a stress guide. The combined data suggest that the upper boundary of the subducted plate, which must be above the BWZ seismicity, lies within a region of low velocity, just above a zone of high velocity gradient. The zone of highest P-wave velocity parallels the BWZ but is located at about 10 km greater depth. Thus, the model suggests lateral variations of up to 10% within the downgoing slab, with the minimum velocity in the uppermost part of the slab corresponding to subducted oceanic crust. The broad negative anomaly beneath the high-velocity slab is interpreted as the asthenosphere underlying the subducted plate.

ZUSAMMENFASSUNG

In den Jahren 1972 bis 1988 wurden vom U.S. Geological Survey und der Universität von Alaska in Fairbanks an über 200 temporären und permanenten seismischen Stationen etwa 15 000 lokale Erdbeben im südlichen Alaska registriert. Im Zusammenhang mit dem Subduktionsprozess der pazifischen Platte unter dem kontinentalen Alaska werden dabei Erdbeben bis in Tiefen von mehr als 200 km beobachtet, obwohl die Mehrheit der Erdbebenherde innerhalb den obersten 60 km liegt. Die gute räumliche Verteilung der Erdbeben und der seismischen Stationen erlauben die Erfassung der dreidimensionalen Struktur der P-Wellengeschwindigkeit der obersten 180 km der Erde mittels der seismischen Tomographie.

---

[1]) Contr. no 628 Institute of Geophysics, ETH Zürich, Switzerland.

[2]) Institute of Geophysics, ETH-Hönggerberg, CH-8093 Zürich, Switzerland.

[3]) U.S. Geological Survey, 345 Middlefield Rd, Menlo Park, CA 94025, USA.

Die Geschwindigkeits-Strukturen innerhalb der Erdkruste (ca. 40 km mächtig) sind in allen erfassten Gebieten mit vergleichbar guter Auflösung ähnlich. Es werden laterale Geschwindigkeitsunterschiede von bis 10% und bis zu 100 km Ausdehnung beobachtet, welche teilweise mit regionalen, geologischen Strukturen korrelierbar sind. Allerdings werden durch die geometrischen Charakteristiken der Parametrisierung (Netzweite von 10 km in allen drei Richtungen) kleinräumige Anomalien von geringeren Amplituden unterdrückt.

Im oberen Mantel werden in allen Tiefenbereichen (50 km bis 180 km) nur wenige, aber grossräumige Geschwindigkeitsanomalien erfasst. Auf Querschnitten ist der geometrische Zusammenhang dieser Anomalien bis in die tiefsten Schichten des Modelles ersichtlich, wobei sich das Bild einer nach WNW gerichteten Subduktionszone ergibt.

Die Verwendung von 10 × 10 × 10 km grossen Blöcken bis in Tiefen von 180 km ermöglicht das Auflösen von Geschwindigkeitsunterschieden der verschiedenen Bereiche innerhalb der subduzierten Lithosphäre. Dabei zeigt sich, dass die Zone grösster P-Wellengeschwindigkeit in der Lithosphäre nicht mit der seismisch aktiven Benioff-Wadati-Zone identisch ist. Vielmehr scheinen diese beiden Zonen parallel zueinander im Abstand von ca. 20 km zu verlaufen. Die seismogene Benioff-Wadati-Zone überdeckt zudem einen Bereich erniedrigter P-Wellengeschwindigkeit.

In Übereinstimmung mit früheren Beobachtungen wird ein Modell vorgeschlagen, welches für die untere Begrenzung der subduzierten Lithosphäre die seismische P-Wellengeschwindigkeit und für die obere Begrenzung die Benioff-Wadati-Zone verwendet. Demnach wäre innerhalb der subduzierten Lithosphäre ein lateraler Geschwindigkeitsgradient von bis zu 10% anzunehmen, wobei die minimalen Geschwindigkeiten mit der teilweise ebenfalls subduzierten ozeanischen Kruste korreliert werden.

Introduction

Southern Alaska is part of the "ring of fire" – the zone of high seismic, volcanic and tectonic activity that circumscribes the Pacific ocean and generally mark an active plate boundary. Here, the oceanic Pacific plate is subducted under the continental North American plate that includes Alaska. In an oceanic lithosphere, as in the Aleutian island arc, this process of subduction most prominently expresses itself by the typical geomorphologic features such as trenches and volcanoes forming an island arc. In southern Alaska the situation is more complex, as the Pacific-North American plate boundary progresses from dextral strike-slip along the Queen Charlotte-Fairweather fault system on the east to underthrusting at the Aleutian megathrust (Lahr & Plafker 1980; Stephens et al. 1984; Page et al. 1989).

The high level of seismic activity together with a large and relatively dense network of seismic stations run by the U.S. Geological Survey, the University of Alaska Geophysical Institute, and the U.S. National Oceanic and Atmospheric Administration (NOAA) Alaska Tsunami Warning Center (Fig. 1) provide an outstanding data set for local earthquake tomography. Hereby the subducting lithospheric slab is not only the cause for earthquakes as deep as 200 km but also the major geologic target of this tomography study that greatly profits from such deep seismic sources.

As a result of the subduction of an oceanic plate that carried several continental fragments southern continental Alaska is made up of accreted terranes of distinct origin (Coney et al. 1980, Ben-Avraham et al. 1981). Ongoing tectonic processes form several young mountain ranges (Stanley et al. 1990) in some places punctuated by active volcanoes. These tectonic and volcanic processes, that occur in a part of the continental plate consisting of a mozaic of different terranes, can be expected to result in a very complex velocity structure. Recent high resolution seismic refraction studies by Flueh et al. (1989) show large lateral variations in the seismic velocity in combination with a surprisingly uniform crustal thickness. Although of great interest, the details

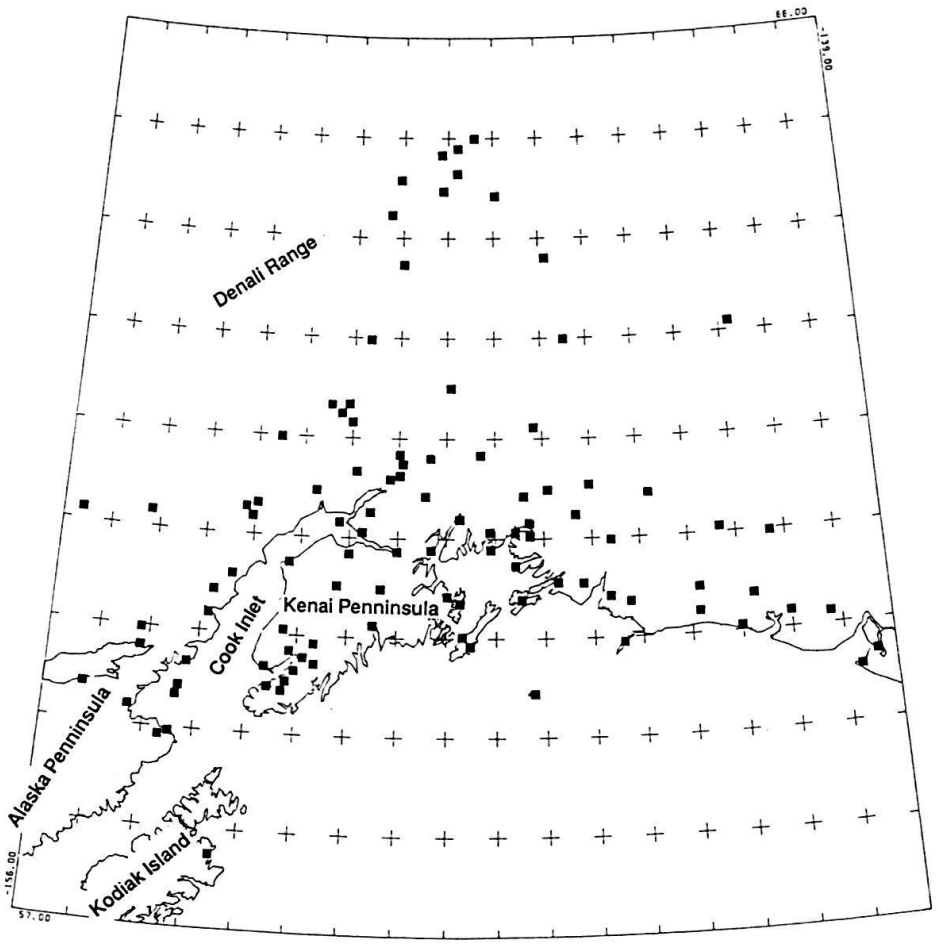

Fig. 1. Seismic network in southern Alaska operated by the U.S. Geological Survey, the University of Alaska Geophysical Institute, and the U.S. National Oceanic and Atmospheric Administration (NOAA) Alaska Tsunami Warning Center: 101 permanent and temporary stations for the time period 1972 through 1988.

of the continental crust in southern Alaska are not the main target of this study but rather complications to be dealt with.

In a seismic tomography study, quantitative and qualitative non-seismic information is of great importance for the interpretation of the three-dimensional velocity field. In southern Alaska, the subducting slab of the Pacific plate forms a prime deep-seated and large target for seismic tomography and has already been studied by other methods (see: ENGDAHL et al. 1977, PAGE et al. 1989). LAHR (1975) inferred the location of the upper surface of this slab from the distribution of earthquakes in the upper mantle that form a bending seismic zone less than 25 km thick. He proposed a maximal extension of the slab up to 64.25° North (some 300 km north of Cook Inlet, Fig. 1). Using a 15 km thick Benioff-Wadati zone (LAHR et al. 1974) for their thermal modeling, ENGDAHL et al. (1977) presented a geometric model of the Pacific slab beneath the Kenai Penninsula and the Cook Inlet (for geographical locations see Fig. 1). According to their model, a cold slab of about 80 km thickness dipping about 60° toward WNW, with P-wave velocities up to 10% higher than standard Earth models

(ENGDAHL & GUBBINS 1987) can be expected. Studies of the recent seismicity (PAGE et al. 1989) confirmed the earlier findings of LAHR et al. (1974). In this study an attempt is made to obtain an image of the 3D P-wave velocity field of the upper mantle in southern Alaska by seismic tomography and to correlate this image with the distribution of hypocenters.

Travel time data

During the period 1972 to 1988, the U.S. Geological Survey, the NOAA Alaska Tsunami Warning Center, and the University of Alaska have operated permanent and temporary seismic stations at 101 sites in Southern Alaska (Fig. 1) and collected some 230,000 P-wave travel time data from about 15,000 local earthquakes. Much of this seismic activity is concentrated along a 150 km wide band parallel to the Cook Inlet and extending inland to the Northeast. For the inversion we used a strict criteria of maximum gap (120°) and minimum number of good P-wave arrivals (10 for the period

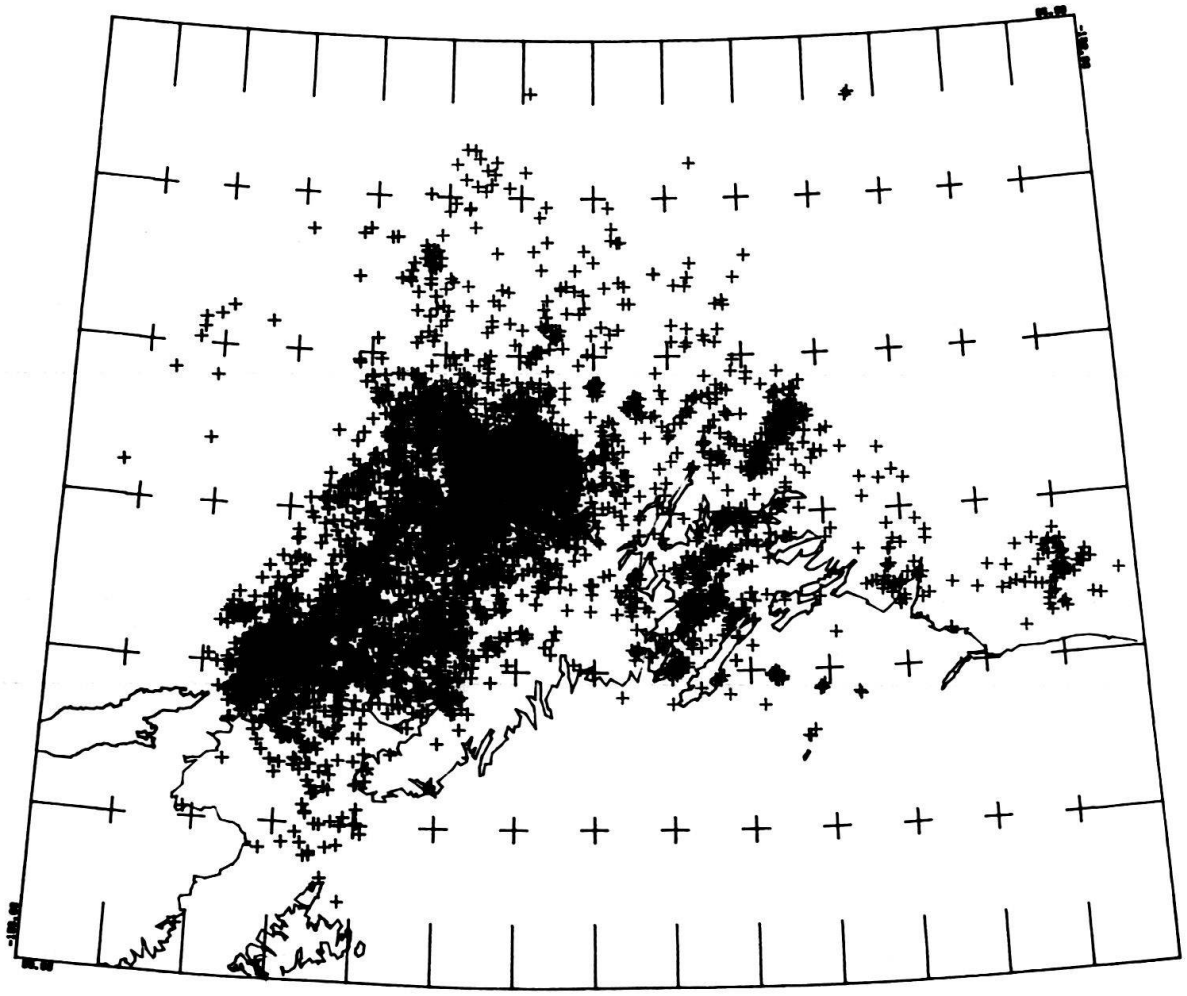

Fig. 2. Epicenter distribution of 4,928 high-quality events in southern Alaska used for this tomographic study. For selection criteria see text.

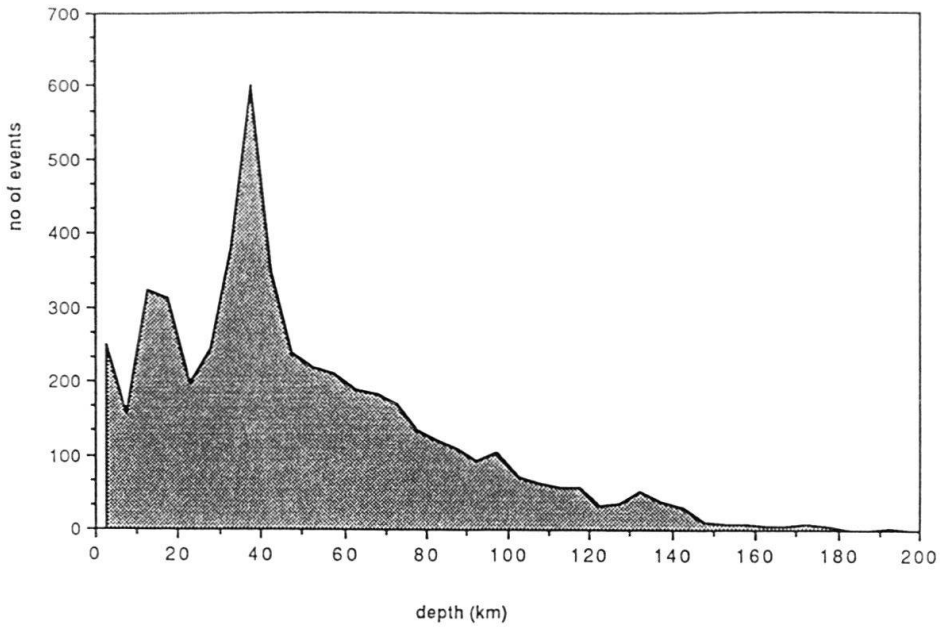

Fig. 3. Depth distribution of 4,928 high-quality events used for tomographic study. The distribution of this subset is very similar to that of the full data set for the time period 1972 through 1988.

1972 to 1985, and 15 for 1986 to 1988) to select a "high quality" data set. The resulting data set consists of over 110,000 P-wave travel times from 4,928 events. These show an epicenter distribution (Fig. 2) similar to that of the original full data set except that most of the events that locate in the Pacific ocean failed the selection criteria. In the depth distribution a maximum is observed (Fig. 3) near 40 km depth. With few events at depths exceeding 150 km the "crossfiring" by rays from earthquakes at such depth is poor and therefore the resolution is reduced at this depth.

Method of inversion

The applied method is an extension of the original ACH-inversion (Aki et al. 1976, Aki & Lee 1976) and has been described in detail by Kissling (1988). The key step in this inversion technique is the direct inversion of an (m) by (m) matrix, where (m) denotes the number of unknown velocity parameters. For computational reasons this limits this technique to a maximum number of about 5,000 unknown model parameters at present. However, after the separation of the roughly 20,000 hypocentral parameters with the high-quality data set of southern Alaska the 3D P-wave velocity field could be resolved either by over 15,000 blocks of 5 km by 5 km by 5 km dimension with fair to good resolution or by about 10,000 blocks of 10 km by 10 km by 10 km size with good to very good resolution. An approximate solution can be calculated for an almost unlimited number of unknowns with a fair degree of accuracy for well resolved blocks (Kissling 1988). The results shown in this paper are calculated with this approximate solution for the ACH-inversion technique for blocks of the sizes 10 km by 10 km by 10 km.

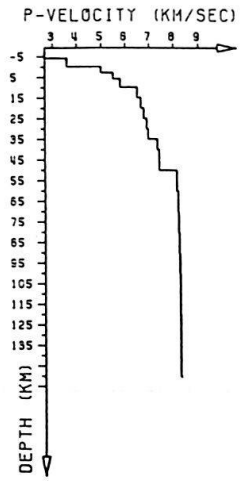

Fig. 4. "Minimum 1D-model" showing the average layer velocities. The velocities derived for this 1D-model reflect only these areas of southern Alaska that were sampled by this data set. The 3D-velocity structures are displayed as percentage velocity deviations relative to each layer velocity in this 1D-model.

Prior to the 3D-model inversion the average layer velocities (Fig. 4) were calculated by a joint inversion of a subset from the high quality earthquake data for hypocentral and 1D-model parameters. This 1D-model with station corrections ("minimum 1D-model", KISSLING 1988) was used to relocate all of the earthquakes prior to the 3D inversion. Tests with data from shots and quarry blasts suggest an accuracy of about 2 km in horizontal and 3 km in vertical direction.

Tomographic results

With blocks of 10 km by 10 km by 10 km the near surface crustal structure cannot be represented adequately. In the middle and lower crust, however, a vertically surprisingly consistent pattern is observed. As a typical example of the crustal structure down to about 50 km depth, layer 4 (40 km to 50 km) is displayed in Fig. 5. In an area of roughly 500 km by 300 km several anomalies of high or low velocity of much smaller extent (from 30 km by 50 km up to 40 km by 100 km) are superimposed on an otherwise fairly uniform P-wave velocity of 7.15 km/s. Most of these anomalies are present in all crustal layers thus forming elongated zones of crust of different average P-wave velocities. In the light of the geologic history a likely interpretation of these zones is a series of wedges of different crust accreted and altered by the subduction process. To test such an interpretation, however, a special study with much finer tomographic crustal blocks set with respect to the surface geology would be necessary.

The appearance of the 3D P-wave velocity field below the depth of the Moho (see Fig. 4) at about 45 km (inferred from refraction seismic results by FLUEH et al. 1989) differs remarkably from anything above the Moho. With the exception of a systematic shift in the location of the most prominent anomalies the overall pattern of the P-wave velocity structure is very similar for all layers between 50 km and 150 km depth. Layer 10 (Fig. 6) represents the depth range of 90 km to 100 km. At this depth three local P-wave velocity anomalies are clearly apparent. Two are elongated SSW-NNE-striking

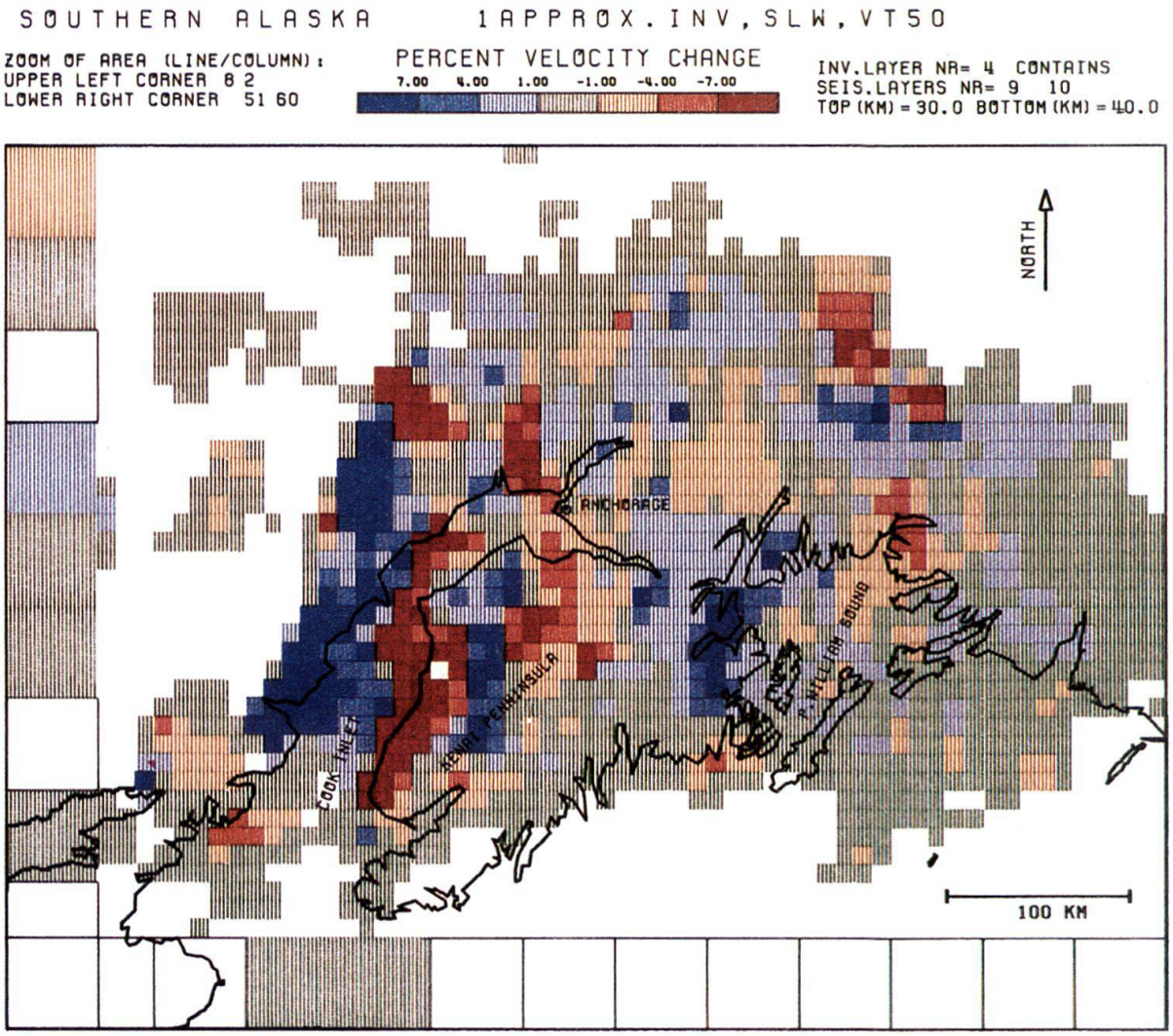

Fig. 5. Lateral variation of P-wave velocity in the depth range 30 km to 40 km in southern Alaska as obtained by approximate ACH-inversion. The lateral variations are calculated as percentage deviations from the average velocity of 7.15 km/s and imaged in blue for areas of higher and in red for areas of lower velocities. The pattern is representative for all crustal layers.

zones of large amplitudes, one of positive and the other of negative sign, and the third is a broad zone of moderately reduced P-wave velocity beneath a large part of the Kenai Penninsula. The last anomaly most likely represents the asthenosphere beneath the oceanic Pacific plate. Relative to the average P-wave velocity in this layer (8.3 km/s), that is dominated because of its larger area by the Alaskan lithosphere, the velocity in the asthenosphere is reduced by 2% to 3%.

The two elongated anomalies of large amplitude belong to a series of similar anomalies occurring between 50 km and 150 km depth and are best viewed in cross sections (profiles 1, 2 and 3) displayed in Figs. 7, 8 and 9, respectively. These three profiles parallel each other with 50 km separation (see Fig. 6), the distance along the profiles being measured from their WNW endpoint. The velocity field is displayed by isolines (lines of equal percent deviation from average layer velocity) where it was sampled by this data set (area marked by crosses) and where the calculated velocity deviates from the average layer velocity by more than 1%. The percent velocity change values of the grid points are calculated by averaging over a 30 km wide band with the center point along the profile given four times the weight of the external points 15 km from the profile.

To enhance the large scale structures hypocenters within a zone of 15 km on either side of the profiles are superimposed onto the velocity field. To keep the systematic errors in the distribution of the hypocenters (shown by open circles) as small as possible only the "high-quality" earthquakes used for tomography are displayed in Figs. 7, 8 and 9. These hypocenters were recalculated by using the 3D-velocity field. An average distance of 2.5 km was observed between the hypocenter locations obtained by use of the 1D-model and those obtained by use of the 3D-model. However, a maximum shift in the hypocenter location of 20 km occurred for an earthquake in the Benioff-Wadati zone (BWZ) at 110 km depth in similar direction as described by Lahr (1975) for earthquakes beneath the Cook Inlet region and by Frohlich et al. (1982) for the Central Aleutian subduction zone. Considering the precision in locating blasts and shots with the 1D-model (see above), we infer a location error of less than 5 km for the majority (over 95%) of the hypocenters.

The three profiles were chosen to illustrate the change in upper mantle structure that occurs between the central and the northern parts of Cook Inlet and Kenai Penninsula. *Profile 1* (Fig. 7) reflects the upper mantle structure found beneath the southern Kenai Penninsula.

With three to four percent reduction the broad anomaly in the upper mantle (distance range of 160 km to 400 km and depth range of 80 km to 150 km) shows the smallest amplitude but is largest in extent. It covers much of the sampled area at depths below 80 km. No earthquakes have been found in this area. There is little doubt that this anomaly reflects the P-wave velocity of the asthenosphere beneath the Pacific lithospheric plate. Above this deep-seated anomalous region is a tilted stack of high-low-high P-wave velocity anomalies. The lower zone of higher than average P-wave velocity dips about 40° toward WNW and has a thickness of roughly 40 km. Its uppermost end reaches to 20 km depth after a change in shape at 50 km depth where it passes through the earthquake zone. At greater depth the earthquakes follow the upper limits of this anomaly while they level out further to the ESE. The lower end of this zone of high P-wave velocity is not reached by this study. This anomaly reflects two different structural bodies. The lower and larger part reflects the subducting Pacific litho-

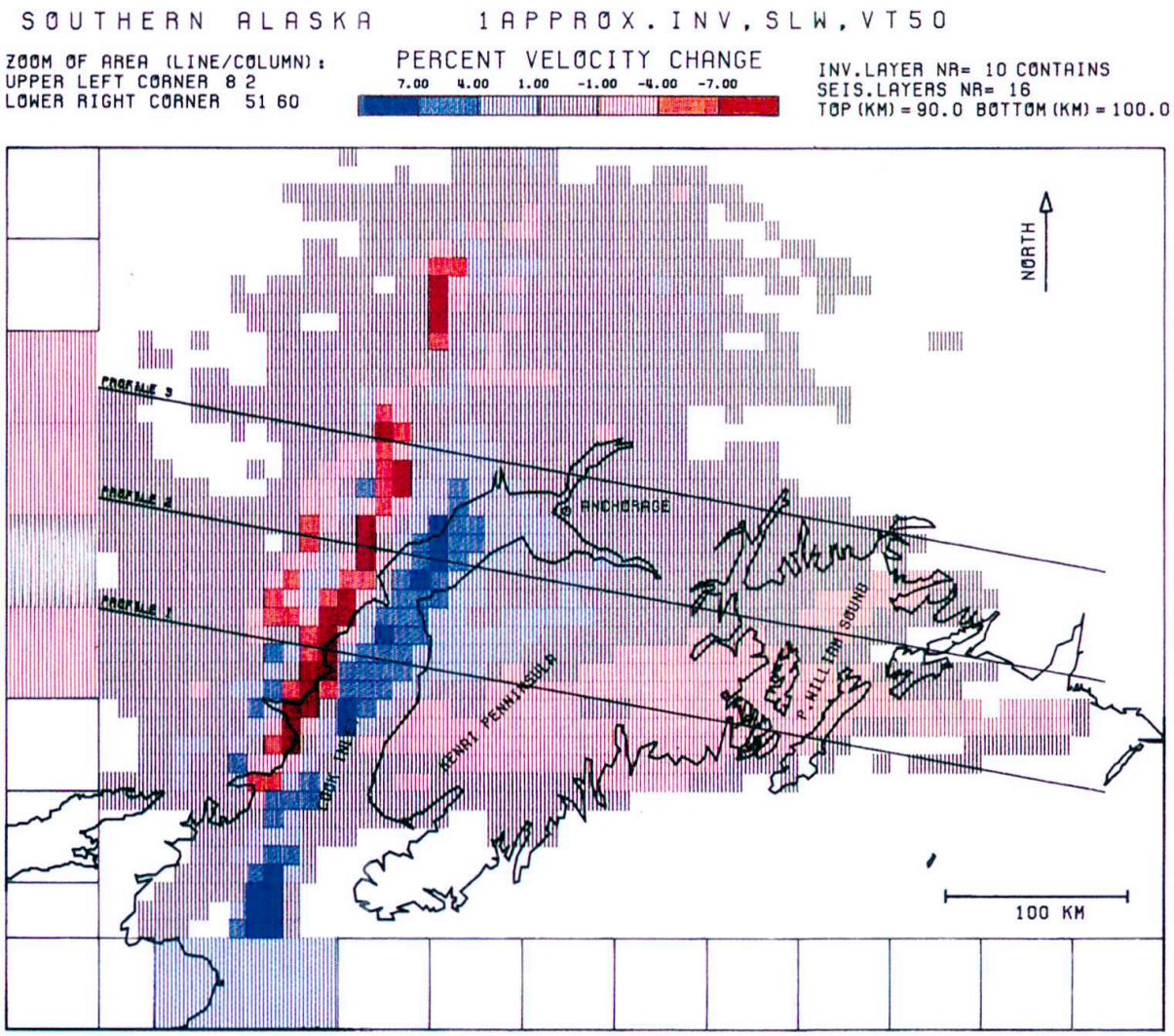

Fig. 6. Lateral variation of P-wave velocity in the depth range 90 km to 100 km in southern Alaska as obtained by approximate ACH-inversion. The lateral variations are calculated as percentage deviations from the average velocity of 8.3 km/s and imaged in blue for areas of higher and in red for areas of lower velocities. The pattern is representative for the depth range 60 km to 150 km. The locations of the cross sections displayed in Figs. 7, 8, 9 are labeled by profiles 1, 2, 3 respectively.

sphere. This tomographic technique (KISSLING 1988) images the velocities as deviations from the average layer velocity in each depth (Fig. 4). Therefore, the subhorizontal part of the Pacific lithosphere beneath Kenai Penninsula that covers two thirds of the profile length in the depth range between 30 km and 70 km is not enhanced as an anomalous region but rather dominates the 1D-model. The upper (crustal) part of the zone of higher P-wave velocity could be interpreted as part of an accreted wedge, but it could also represent an artifact due to "leakage" from the zone below. In the distance range of 90 km to 210 km two zones of anomalous velocity reach from the surface to depths of 90 km (the high velocity anomaly) and to depths exceeding 110 km (zone of lower velocity). The increase or decrease in the P-wave velocity in both cases is about 10%. The subvertical zone of higher velocity coincides more or less with the well resolved part of the continental Alaskan lithosphere. In combination with the high velocity slab of the subducting Pacific lithosphere the latter two regions of anomalous P-wave velocity form a sequence of positive-negative-positive velocity anomalies that may be observed, with variations, in all three profiles. The strongest lateral velocity gradient with changes of 13% over a distance of 20 km is observed all along the Benioff-Wadati zone.

In *profile 2* (Fig. 8) there is a well-developed high-velocity slab down to a depth of about 140 km beneath a 40 km thick and extensive zone of reduced velocity. The broad zone of low velocity underlying the high-velocity slab in Fig. 7 that was interpreted as the asthenosphere is reduced in size and in amplitude in profile 2. The subhorizontal high-velocity zone underlies most of Kenai Penninsula and continues after a smooth bend with a dip of about 30 degrees beneath Cook Inlet to a depth of 130 km. In contrast to profile 1 (Fig. 7) the near-surface local anomaly of high P-wave velocities below the NW Kenai Penninsula do not connect with this high-velocity slab. The majority of the earthquakes are located in clusters in the crust and along the zone of high velocity gradient. Few events occur within the high-velocity slab.

In *profile 3* (Fig. 9) the high-velocity slab is reduced to a subhorizontal zone, slightly bent at its NW end, underlying a thinner low-velocity zone that is remarkably reduced in amplitude when compared with profile 1 (Fig. 7). Of all three profiles, the high-velocity slab underlying profile 3 is smallest in extent and weakest in amplitude.

The direction of the profiles (Figs. 7, 8 and 9) was chosen to view the maximum dip angle of the subducting lithosphere and is approximately perpendicular to the strike of the subduction zone beneath Cook Inlet. With 40 to 45 degrees (Fig. 7) the dip angle of the high velocity subducting lithosphere is in good agreement with rheological models for the Aleutian subduction zone (HAGER & O'CONNELL 1978). The BWZ (PULPAN & FROHLICH 1985) and the high velocity slab parallel each other and therefore the estimate of the dip angle is not affected by the discussion of the upper bounds of the subducting lithosphere (see below).

The interpretation of a tomographic image based on relative velocity anomalies is ambiguous, last but not least for the reason that a single zone of anomalous P-wave velocity may reflect more than one local chemical or thermal anomaly or even is a representation of a mixture of both. In a subduction zone the latter is very likely. As a schematic illustration of such effects Fig. 10 shows a hypothetical tomographic image of a cross section across the subduction zone of western Canada, simplified after DREW & CLOWES (1990). The zone of strongly reduced P-wave anomaly along the

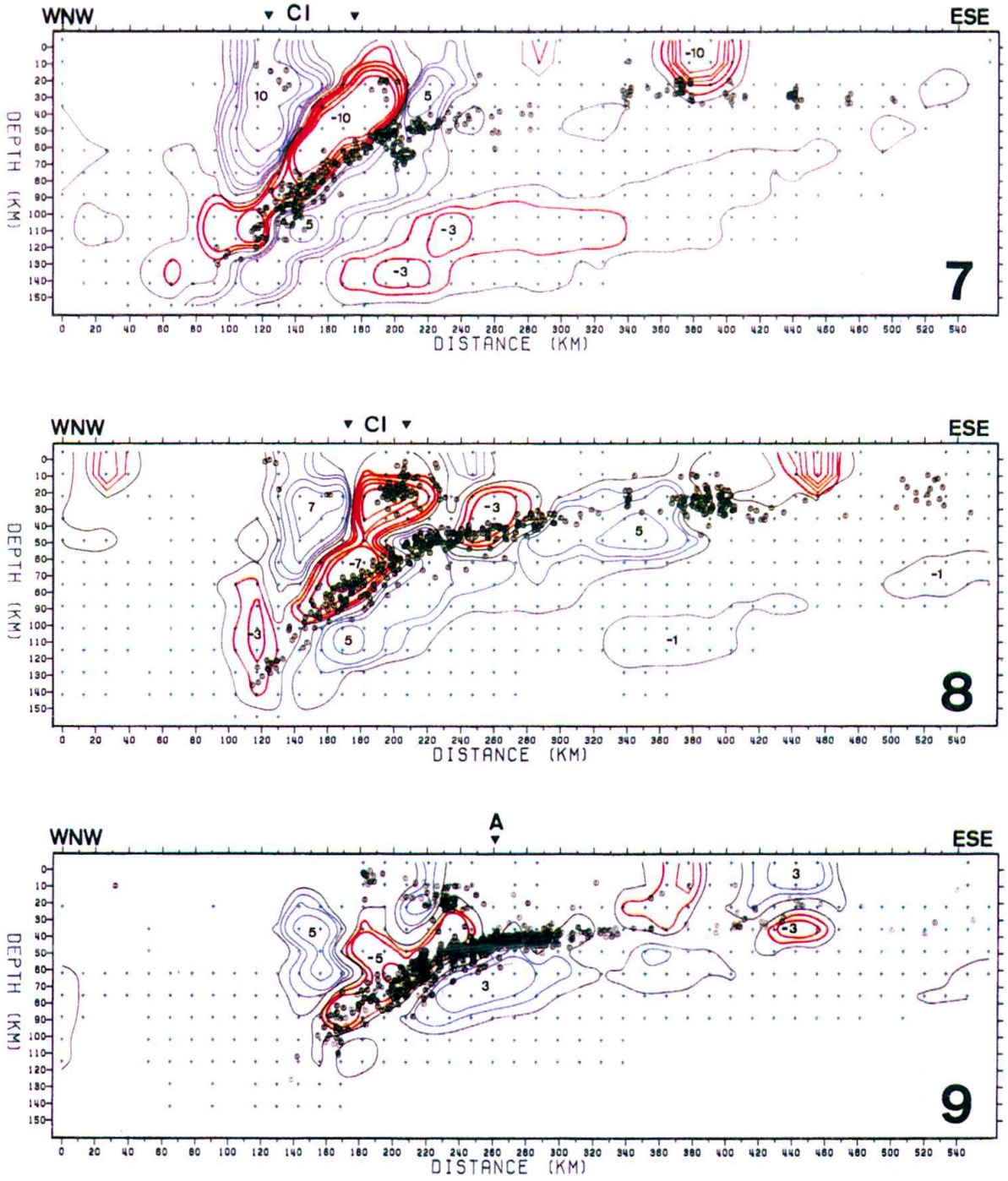

Figs. 7, 8 and 9 (from bottom to top): Cross section of 3D P-wave velocity structure in southern Alaska along profiles 1 (south, Fig. 7), 2 (middle, Fig. 8) and 3 (north, Fig. 9) (see Fig. 6 for location). As geographical markers the location of Cook Inlet (CI) and Anchorage (A, 15 km to the south) are given. The cross sections are plotted with no vertical exaggeration. The area that was sampled by the current data set has been marked by crosses. The isolines of velocity variations are calculated as percentage deviations from the average layer velocities with little smoothing by the interpolation process (see text) and imaged in blue for areas of higher and in red for areas of lower velocities than the respective average layer velocity. Contouring intervals are −10%, −7%, −5%, −3%, −2% in red, −1% and 1% in black, and 2%, 3%, 5%, 7% in blue. The numbers in the figures denote the maximum and minimum values in percent. Hypocenters (open circles) of the high-quality data set within 15 km of the profiles were projected perpendicular to the profile plane.

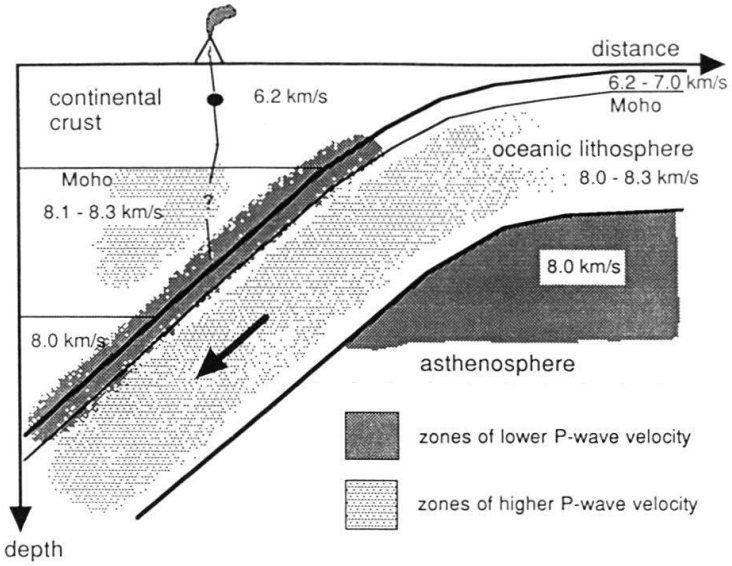

Fig. 10. Interpretation of a tomographic image: Schematic vertical cross section through a continent-ocean subduction zone following the seismic model of Drew & Clowes (1990) for the subduction zone of western Canada with the tomographic image of such a velocity structure superimposed. The velocity anomalies shown are relative to average velocities in each depth interval, i.e., relative to a 1D-model, as imaged by local earthquake tomography.

upper part of the subducting lithosphere is in part caused by the low-velocity oceanic crust (low velocity relative to the P-wave velocity of the upper mantle material in the same depth). The subduction of oceanic crust may lead to the existence of partial melts and alter the contact zone resulting in a reduced velocity in the wedge.

Stress regime in a subducted plate

During the time span of January 1972 and December 1988 within the Cook Inlet region (latitude 59 to 63 degrees north, longitude 148 to 156 degrees west, see Fig. 11A) 10,968 earthquakes were recorded which meet the following conditions:

no. of P arrivals 6 or more, no. of S arrivals 2 or more, RMS-value ≤ 0.7 and a location quality value Q (Lee & Lahr 1975) of A, B or C.

Each of these events has been assigned coordinates (Fig. 11A) according to where its epicenter falls within the Cook Inlet region (CX, CS) and according to where the event lies (Fig. 11B) with respect to a reference Benioff-Wadati zone surface (SD, SZ). The reference BWZ surface was defined to approximate the upper bound of the BWZ beneath Cook Inlet. Next the 1,447 events with (CS) coordinates between 0 and 100 km and with (SZ) coordinates between 0 and 30 km were selected. These events were divided into ten groups, lettered (a) through (j), according to their (SD) coordinate, and composite focal mechanisms were computed for each group (Fig. 12). Note that the focal mechanisms have back plane projection on a plane parallel to the cross section of Fig. 11B. As an example, the larger focal sphere of Fig. 12B shows the composite focal mechanism for the group (b), based on all first motions recorded from events within this group. The smaller focal sphere shows the distribution of P and T

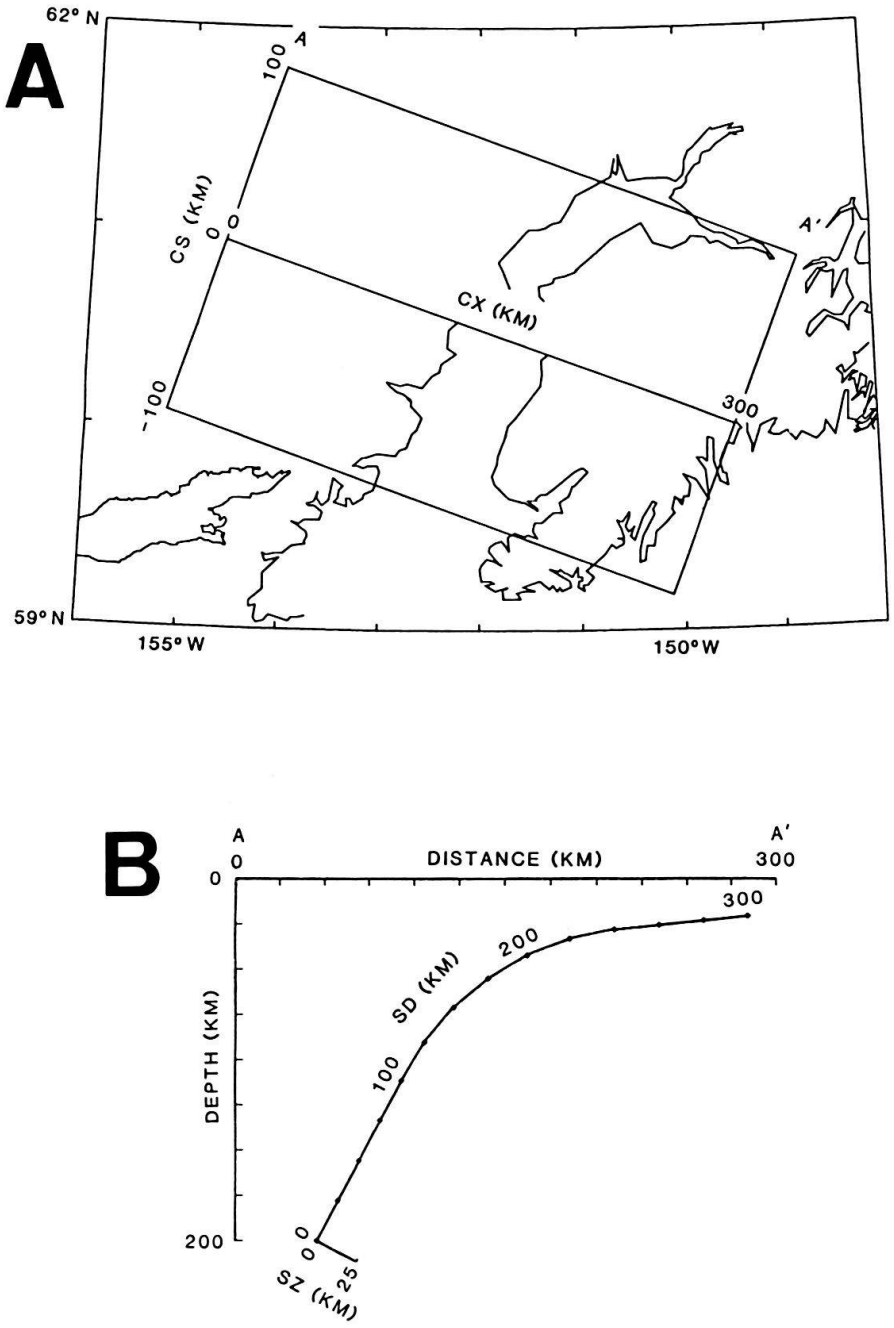

Fig. 11. Coordinate system for Benioff-Wadati zone beneath Cook Inlet. Upper part (A): Rotated coordinates (CX, CS) at Earth's surface. (CX) parallel to cross section AA'. (CS) distance from cross section at CS = 0. Lower part (B): Cross section AA' with (SD, SZ) coordinates along Benioff-Wadati zone.

axes that best fit this data. The P and T axes reflect the directions of greatest and least compressive stress. In Fig. 12A the directions of the T-axis (lines across each circle) for all ten groups of the BWZ are given. Note that the T-axes for all of the groups fall close to the plane of the cross section and that the orientation of this axis tends to parallel the seismic zone. This is consistent with the plate being pulled into the asthenosphere by gravitational forces, and acting as a stress guide. The inplane tensional

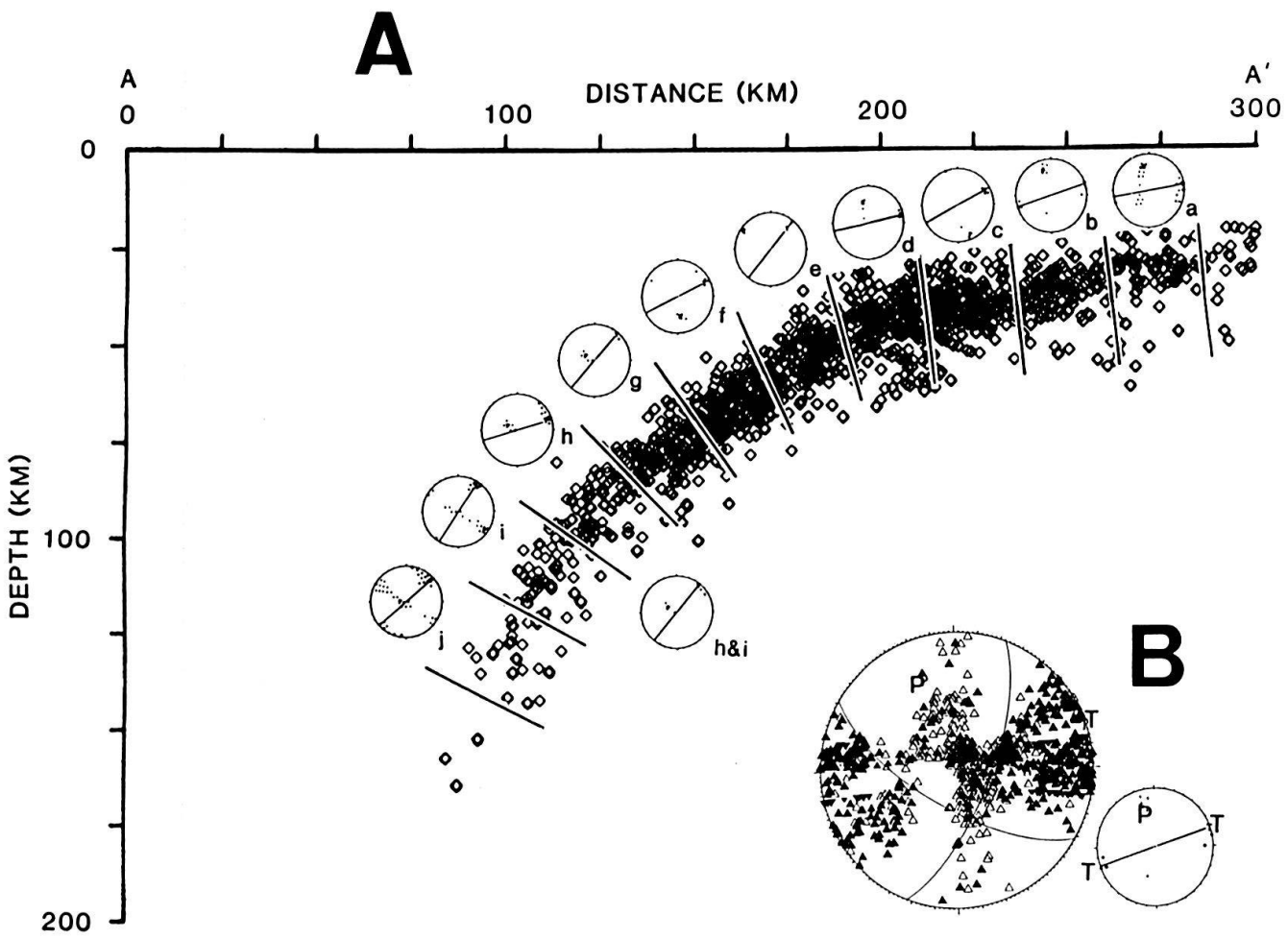

Fig. 12. A: Cross section of Benioff-Wadati zone (BWZ) beneath Cook Inlet with composite focal mechanisms for ten sections of the BWZ (lettered a through j). The cross section includes 1,447 events with coordinates 0 km < CS < 100 km (see Fig. 11) and 0 km < SZ < 30 km within the BWZ. Note that the T-axes for all of the ten groups fall close to the plane of the cross section and that the orientation of this axis tends to parallel the BWZ. The dots in the small circles represent the P and T axes (see explanation below). B: Composite focal mechanism for group (b) with all first motions (open triangles denote dilatation, solid triangles compression) in a back plane projection on a plane parallel to the cross section of Fig. 12A. The directions of the maximum compressive stress and of the maximum tensile stress are marked by P and T, respectively. The smaller circle summarizes the results for the group (b) by displaying the T-axis by a cross line and the P-axis by the letter P.

stress regime continues within the gently dipping Aleutian BWZ to the northeast (PAGE et al. 1989).

Although less well constrained, the P-axes tend to be oriented perpendicular to the BWZ in sections (a) through (f), and then to be oriented parallel to the strike of the zone. PULPAN & FROHLICH (1985) summarized the BWZ focal mechanisms for events just to the south (between 59 and 60.5 N and deeper than 50 km) and noted that the P-axes fell within 25 degrees of a north-south horizontal axis. Compression within the deeper portion of the BWZ beneath Cook Inlet might be expected due to the linearity of this portion of the zone (FRANK 1968).

In our opinion, the consistent pattern of the T-axis around the downward bending BWZ supports the hypothesis that all of these earthquakes (Fig. 12A) occur within a contiguous plate and that they outline the upper bound of subducting lithosphere. This point will be of importance for the interpretation of the velocity structure independently obtained by seismic tomography.

Discussion

It is a commonly accepted model of subduction zones that the Benioff-Wadati zone formed by the deeper earthquakes is confined to the subducting plate (ENGDAHL et al. 1989, Fig. 3). This seems plausible as the subducting slab would be more rigid than the surrounding asthenosphere. With such a definition, a model of the slab is entirely based on the geometric distribution of earthquakes. Physical arguments suggest that the lithospheric slab should have a lower temperature (with the exception of a narrow zone heated by friction) and a higher seismic velocity than the surrounding asthenosphere.

By inversion of teleseismic data ENGDAHL et al. (1977) and ENGDAHL & GUBBINS (1987) for the Aleutian Islands, HIRAHARA (1980, 1981 and 1988) and HIRAHARA & MIKUMO (1980) for Japan, and BOLDYREV (1985) for Kamchatka obtained images of the P-wave velocity distribution in subduction zones. With a high-velocity slab of up to 5% velocity deviation overlayed by a zone of reduced P-wave velocity our results match their general findings. Due to the characteristics of the data (local earthquakes for this study versus teleseismic data for most of theirs) the tomographic image of the slab is limited in depth to about 180 km but has much higher spatial resolution. While much of the general geometry of the subduction zone in southern Alaska has been described by earlier studies (see above) some structural details that were made visible by local earthquake tomography may lead to a refined model of the subduction process. In particular, the velocity structure of the Alaskan lithosphere seems to have been significantly altered by the impact of the subduction process.

In the last decade several seismic tomography studies (see, f.e., BOLDYREV 1985; HASEMI et al. 1984) have used local earthquakes or a combination of local earthquake and teleseismic data to derive seismic images of the wedge. BOLDYREV (1985) for the region of Kamchatka made observations similar to ours with respect to the geometrical relation between the seismically active region and the P-wave velocity structure of the subduction zone. HASEMI et al. (1984) obtained a somewhat different seismic image of the wedge material in the depth range 30 km to 70 km beneath the volcanic front of Japan. Generally, the velocity structure in the upper mantle above the descending

lithosphere in Japan is rather uniform with a minor reduction in P-wave velocity in the depth of 30 km to 70 km beneath the volcanic regions.

In all three cross sections (Figs. 7, 8 and 9) the P-wave velocity anomaly with the largest amplitude and extent is a zone of reduced velocity. This zone lies partly above the Benioff-Wadati seismogenic zone and also above the zone of relative high-velocity that can be interpreted as the descending lithospheric slab. CHIU et al. (1985) found evidence for "a deep magma source right above the upper surface of the descending lithosphere beneath the active volcanoes on Tanna Island", and their results would indicate that such a zone also extends updip along the slab. With reference to the model of DREW & CLOWES (1990) for the subduction zone of western Canada (Fig. 10) the low velocity zone along the upper surface of the slab could in parts be interpreted as remnants of the subducted oceanic crust. While a relative high temperature up to partial melting seems a plausible reason for the reduction in the velocity, the causes of such a temperature-pressure regime in the zone of high seismic activity (BWZ) are debatable (ROBINSON 1983). In profile 1 (Fig. 7) the subduction zone seems to be fully developed with the high-velocity slab reaching deeper than the maximum resolved depth whereas the zone of strongly reduced velocity does not reach much deeper than 110 km. This could correlate with the thickness of the continental lithosphere. It is interesting to note that many of the active volcanoes along the Cook Inlet and the southern shore of the Alaskan Penninsula are situated above the deepest part of the zone of strongly reduced velocity.

However, a direct connection between this deepest part of the velocity anomaly and the volcanoes cannot be drawn as there is an intervening volume of high P-wave velocity which is 30 km wide and over 90 km deep. Either conduits for heat transfer to the active volcanoes exist within this subvertical zone of higher P-wave velocity or the volcanoes reflect melting in the overlying wedge (KUSHIRO 1987). Obviously, with block sizes of 10 km by 10 km by 10 km the tomographic image presented here cannot resolve such a narrow feature. Certainly, a detailed image of the velocity structure in the wedge is essential for a better understanding of the magma generation which feeds volcanoes. A special tomographic study with reduced block size and the use of S-wave (see f.e., HIRAHARA 1980) and amplitude data to enhance more details of the P- and S-wave velocity structure in the overriding continental lithosphere might prove useful. Independent high-resolution information about other physical rock parameters in connection with petrophysical arguments and contraints are also necessary to interpret the two elongated high amplitude P-wave velocity anomalies in the wedge (Fig. 7, velocity anomalies beneath Cook Inlet [CI]).

The hypocenters map out a well defined BWZ beneath Cook Inlet (Fig. 12) that strikes parallel to the volcanic arc and reaches about 100 km depth beneath the volcanoes. The focal mechanisms are consistent with the hypothesis that all of the BWZ activity comes from within the subducted plate, and that shear parallel to the surface of the subducted plate is not a predominant mechanism. The velocity inversion results indicate a strong gradient in P-wave velocity throughout the seismogenic zone along the upper portion of the subducted plate.

The geometric relation between the Benioff-Wadati zone and the upper bounds of the high-velocity zone raises some questions about the definition of the geometrical extent of a subducting lithospheric slab. In profile 1 (Fig. 7) the tomographic image is

almost identical to the results presented by ENGDAHL & GUBBINS (1987) for the Aleutian subduction zone, thus, supporting a model by CHIU et al. (1985) that "the intermediate-depth earthquakes probably occur mainly outside the cold high velocity elastic core of the descending lithosphere [CHAPPLE & FORSYTH 1979] in a zone where thermal and velocity gradients are highest." CHIU et al. (1985) measured apparent P-wave velocities of 7.7 km/s and 6.9 km/s for waves travelling in the upper part of the descending lithospheric slab from earthquakes at about 170 km depth in the Vanuatu arc region. Compared with the P-wave velocities obtained by this tomographic study the second value seems somewhat low while a P-wave velocity of 7.7 km/s represents an average value for a good part of the zone of reduced P-wave velocity in profile 1 (Fig. 7) directly above the high-velocity slab. The two apparent velocities given by CHIU et al. (1985) were derived from phases refracted by the still faster inner part of the slab, suggesting that these rays did not necessarily sample the fastest portion of the slab in its full length. Our tomographic results support such an interpretation.

Thus, in accordance with the model by CHIU et al. (1985, Fig. 11B) our results suggest, that a good part of the zone of reduced P-wave velocity in Fig. 7 belongs to the subducting lithospheric slab. Neither the geometric distribution of the earthquakes nor the 3D P-wave velocity structure unambiguously outline the bounds of the subducting lithosphere. Considering the effects on the location of intermediate depth earthquakes (FROHLICH et al. 1982, and this study) by use of a 3D-velocity model rather than a standard 1D-model the outline of the BWZ is well defined (location errors smaller than 5 km on average). Likewise, the zone of low velocity that partly overlaps the BWZ and that parallels the subducting high velocity slab is a well resolved, broad feature of high amplitude, which can also be regarded as geometrically well defined. This leads to the conclusions, that

– a large number of BWZ earthquakes occur in a zone of relatively low P-wave velocity, and that

– the upper bound of the subducting lithosphere cannot be defined on the basis of the P-wave velocity structure, since the zone of reduced velocity in the wedge and the low velocity zone of the subducting oceanic crust form a continuous, large area of lower P-wave velocity. This is in contrast to the findings of HIRAHARA & MIKUMO (1980, p. 118) who observed a sharp velocity contrast at the upper plate boundary for the subduction of the Pacific plate under Japan.

Defining the upper plate boundary by the upper limits of the BWZ and the lower plate boundary by the contrast in P-wave velocity between the high-velocity subducting slab and the underlying asthenosphere (this in accordance with HIRAHARA & MIKUMO 1980), we observe a thickness of the descending lithosphere of about 50 km. Further work is planned to test and confirm the apparent relative offset between the BWZ and the high-velocity anomaly, although no reason for such a location bias is known at this time.

Considering the differences in the average block size between the work of HIRAHARA & MIKUMO (1980) and BOLDYREV (1985) and this study, the broad features in the tomographic image of the subduction zone in southern Alaska confirm and the details of the velocity structure complement the earlier findings. The use of an extraordinary set of local earthquake data permit the illumination of many details (structures of 15 km to 20 km size could be resolved) of the velocity structure of the uppermost

150 km. For the internal structure of the subducted lithospheric slab and for its upper mantle environment this may be a sufficiently detailed image. The same resolution, however, is inadequate to model the details of the wedge above the subducting lithosphere and grossly inadequate to illuminate crustal scale velocity anomalies or even magma chambers and diapirs. Additional tomographic studies are necessary with smaller block sizes for the wedge and crust and with teleseismic data to resolve the velocity structure of the subduction zone at greater depth.

The characteristics of the approximate inverse solution (KISSLING 1988) must caution any speculative interpretation of small-sized local anomalies at this stage. However, as inversion tests with artificial data (KISSLING 1988), compatible with the quality of this local earthquake data set have shown, the general features of the tomographic model of the 3D P-wave velocity field are well resolved.

Acknowledgments

We thank the NOAA Alaska Tsunami Warning Center and the University of Alaska Geophysical Institute for sharing their seismic data. For several fruitful discussions and suggestions we thank R. Freeman, D. Mayer-Rosa and B. Martinelli (ETH Zürich, Switzerland). We are indebted to W.L. Ellsworth (USGS, Menlo Park, California) and A.B. Thompson (ETH Zürich, Switzerland) for their suggestions in the process of reviewing the manuscript.

REFERENCES

AKI, K. & LEE, W.H.K. 1976: Determination of three-dimensional velocity anomalies under a seismic array using first P-arrival times from local earthquakes, 1, A homogeneous initial model. J. Geophys. Res. 81, 4381–4399.

AKI, K., CHRISTOFFERSSON, A. & HUSEBYE, E.S. 1976: Three-dimensional seismic structure of the lithosphere under Montana LASA, Bull. Seismol. Soc. Am. 66, 501–524.

BEN-AVRAHAM, Z., NUR, A., JONES, D.L. & COX, A. 1981: Continental accretion: From oceanic plateaus to allochthonous terranes. Science 213/4503, 47–54.

BOLDYREV, S.A. 1985: Mantle heterogeneities within active margins of the world oceans and their seismological characteristics. Tectonophysics 112, 255–276.

CONEY, P.J., JONES, D.L. & MONGER, J.W.H. 1980: Cordilleran suspect terranes. Nature 288/5789, 329–333.

CHAPPLE, W.M. & FORSYTH, D.W. 1979: Earthquakes and bending of plates at trenches. J. Geophys. Res. 84, 6729–6749.

CHIU, J.-M., ISACKS, B.L. & CARDWELL, R.K. 1985: Propagation of high-frequency seismic waves inside the subducted lithosphere from intermediate-depth earthquakes recorded in the Vanuatu arc. J. Geophys. Res. 90, 741–754.

DREW, J.J. & CLOWES, R.M. 1990: A re-interpretation of the seismic structure across the active subduction zone of western Canada. In: Studies of laterally heterogeneous structures using seismic refraction and reflection data. (Ed. by GREEN, A.G.). Geol. Survey Canada, paper 89–13, 115–132.

ENGDAHL, E.R., SLEEP, N.H. & LIN, Ming-te 1977: Plate effects in North Pacific subduction zones. Tectonophysics 37, 95–116.

ENGDAHL, E.R. & GUBBINS, D. 1987: Simultaneous travel time inversion for earthquake location and subduction zone structure in the central Aleutian Islands. J. Geophys. Res. 92, 13855–13862.

ENGDAHL, E.R., BILLINGTON, S. & KISSLINGER, C. 1989: Teleseismically recorded seismicity before and after the May 7, 1986, Andreanof Islands, Alaska, earthquake. J. Geophys. Res. 94, 15481–15498.

FLUEH, E.R., MOONEY, W.D., FUIS, G.S. & AMBOS, E.L. 1989: Crustal structure of the Chugach mountains, Southern Alaska: A study of peg-leg multiples from a low-velocity zone. J. Geophys. Res. 94/B11, 16023–16035.

FRANK, F.C. 1968: Curvature of island arcs. Nature 220, 363.

Frohlich, C., Billington, S., Engdahl, E.R. & Malahoff, A. 1982: Detection and location of earthquakes in the Central Aleutian subduction zones using island and ocean bottom seismograph stations. J. Geophys. Res. 87/B8, 6853–6864.

Hager, B.H. & O'Connell, R.J. 1978: Subduction zone dip angles and flow driven by plate motion. Tectonophysics 50, 111–133.

Hasemi, A.H., Ishii, H. & Takagi, A. 1984: Fine structure beneath the Tohoku district, northeastern Japan arc, as derived by an inversion of P-wave arrival times from local earthquakes. Tectonophysics 101, 245–265.

Hirahara, K. 1980: Three-dimensional shear velocity structure beneath the Japan Islands and its tectonic implications. J. Phys. Earth 28, 221–241.

— 1981: Three-dimensional seismic structure beneath Southwest Japan: the subducting Philippine sea plate. Tectonophysics 79, 1–44.

— 1988: Detection of three-dimensional velocity anisotropy. Phys. Earth Plan. Inter. 51, 71–85.

Hirahara, K. & Mikumo, T. 1980: Three-dimensional seismic structure of subducting lithospheric plates under the Japan Islands. Phys. Earth Plan. Inter. 21, 109–119.

Kissling, E. 1988: Geotomography with local earthquake data. Rev. Geophys. 26, 659–698.

Kushiro, I. 1987: A petrological model of the mantle wedge and lower crust in the Japanese island arcs. In: Magmatic Processes: Physicochemical Principles. (Ed. by Mysen, B.O.). Geochemical Soc. spec. publ. 1, 165–181, Washington.

Lahr, J.C. 1975: Detailed seismic investigation of Pacific-North American plate interaction in South Alaska. Ph.D. thesis, New York, Columbia University.

Lahr, J.C., Engdahl, E.R. & Page, R.A. 1974: Location and focal mechanisms of intermediate depth earthquakes below Cook Inlet. Trans. Am. Geophys. Union, 55, 349 (abstract).

Lahr, J.C. & Plafker, G. 1980: Holocene Pacific-North American plate interaction in southern Alaska: Implications for the Yakataga seismic gap. Geology 8, 483–486.

Lee, W.H.K. & Lahr, J.C. 1975: HYPO71: A computer program for determining hypocenter, magnitude, and first motion pattern of local earthquakes. U.S. Geol. Survey Open-file rep. 75–311.

Page, R.A., Stephens, C.D. & Lahr, J.C. 1989: Seismicity of the Wrangell and Aleutian Wadati-Benioff zones and the North American plate along the Trans-Alaska crustal Transect, Chugach Mountains and Copper River basin, Southern Alaska. J. Geophys. Res. 94, 16059–16082.

Pulpan, H. & Frohlich, C. 1985: Geometry of the subducted plate near Kodiak island and lower Cook Inlet, Alaska, determined from relocated earthquake hypocenters. Seism. Soc. Am. Bull. 75, 791–810.

Robinson, R. 1983: Velocity structure of the Wellington region, New Zealand, from local earthquake data and its implications for subduction tectonics. Geophys. J.R. astron. Soc. 75, 335–359.

Stanley, W.D., Labson, V.F., Nokleberg, W.J., Csejtey, B. Jr. & Fisher, M.A. 1990: The Denali fault system and Alaska Range of Alaska: Evidence for underplated Mesozoic flysch from magnetotelluric surveys. Geol. Soc. Am. Bull. 102, 160–173.

Stephens, C.D., Folgeman, K.A., Lahr, J.C. & Page, R.A. 1984: Wrangell Benioff zone, southern Alaska. Geology 12, 373–376.

Manuscript received 28 October 1990
Revision accepted 5 March 1991